RADIOPHYSICS

Original article
DOI: https://doi.org/10.18721/JPM.16309

DESCRIPTION OF POLARIZATION-MAINTAINING FIBERS IN ANALYZING THE PRACTICAL FIBER-OPTIC CIRCUITS USING THE JONES FORMALISM

V. S. Temkina✉, *L. B. Liokumovich, A. B. Archelkov, I. R. Buchilko, A. V. Medvedev, A. V. Petrov*

Peter the Great St. Petersburg Polytechnic University, St. Petersburg, Russia

✉ temkina_vs@spbstu.ru

Abstract. In this paper, analytical forms of the Jones matrix of a polarization-maintaining (PM) optical fiber have been obtained, taking into account a slight deviation of the real fiber of this type from its ideal representation by the linear phase plate model. The derivation was made within the framework of the polarization element model with phase anisotropy. The features of using different variants of matrices in simulation were considered. The results could be used to describe practical fiber-optic circuits with PM fibers, simulate their signal, and analyze the effect of polarization mismatches in the circuits' work. The experiments revealing deviations of the parameters of the polarization modes of real PM fibers from the idealized model and allowing estimation of the level of this deviation were performed.

Keywords: Jones formalism, polarization-maintaining fiber, phase anisotropy, polarization state of light

Funding: The reported study was funded by Russian Science Foundation Grant No. 22-19-00513 (https://rscf.ru/en/project/22-19-00513/)

Citation: Temkina V. S., Liokumovich L. B., Archelkov A. B., Buchilko I. R., Medvedev A. V., Petrov A. V., Description of polarization-maintaining fibers in analyzing the practical fiber-optic circuits using the Jones formalism, St. Petersburg State Polytechnical University Journal. Physics and Mathematics. 16 (3) (2023) 95–114. DOI: https://doi.org/10.18721/JPM.16309

Научная статья
УДК 535.5, 535-4, 535.012.2
DOI: https://doi.org/10.18721/JPM.16309

ОПИСАНИЕ ВОЛОКОННЫХ СВЕТОВОДОВ С ЛИНЕЙНЫМ ДВУЛУЧЕПРЕЛОМЛЕНИЕМ ПРИ АНАЛИЗЕ ПРАКТИЧЕСКИХ ОПТОВОЛОКОННЫХ СХЕМ МЕТОДОМ ВЕКТОРОВ И МАТРИЦ ДЖОНСА

В. С. Темкина✉, *Л. Б. Лиокумович*, *А. Б. Арчелков*, *И. Р. Бучилко*, *А. В. Медведев*, *А. В. Петров*

Санкт-Петербургский политехнический университет Петра Великого, Санкт-Петербург, Россия

✉ temkina_vs@spbstu.ru

Аннотация. В работе получены выражения для матрицы Джонса волоконного световода с линейным двулучепреломлением (ДЛП-волокно), которые учитывают слабое отклонение реального волокна такого типа от его идеального представления моделью линейной фазовой пластинки. Вывод проведен в рамках модели поляризационного элемента с фазовой анизотропией. Рассмотрены особенности использования разных вариантов матриц при моделировании оптоволоконных схем. Результаты могут быть использованы для описания практических оптоволоконных схем с ДЛП-волокнами, моделирования сигнала таких схем и анализа влияния на их работу поляризационных рассогласований. Выполнены эксперименты, которые выявили отклонение параметров поляризационных мод реальных ДЛП-волокон от идеализированной модели и позволили оценить уровень этого отклонения.

Ключевые слова: формализм Джонса, двулучепреломляющее оптоволокно, фазовая анизотропия, состояние поляризации света

Финансирование: Исследование выполнено за счет гранта Российского научного фонда № 00513-19-22 (https://rscf.ru/project/22-19-00513/)

Ссылка для цитирования: Темкина В. С., Лиокумович Л. Б., Арчелков А. Б., Бучилко И. Р., Медведев А. В., Петров А. В. Описание волоконных световодов с линейным двулучепреломлением при анализе практических оптоволоконных схем методом векторов и матриц Джонса // Научно-технические ведомости СПбГПУ. Физико-математические науки. 2023. Т. 16. № 3. С. 95–114. DOI: https://doi.org/10.18721/JPM.16309

Introduction

The paper considers birefringent optical fibers, achieving significant linear anisotropy by means of a special transverse structure. These fibers are widely known as polarization-maintaining (PM) in foreign literature. Linear anisotropy consists of propagation of two linearly polarized modes in orthogonal directions in the optical fiber. PM fibers are used in fiber-optic circuits along with other elements of polarization optics to provide reliable transformation of polarization state of light propagating in the circuit. This may be necessary to reduce fluctuations or fading of signal parameters generated in the optical circuit.

In other cases, the performance of the device to be constructed relies on a certain sequence of transformation of the polarization state. Since polarized light is typically used for this purpose, analysis of such circuits with respect to polarization (including analysis of polarization mismatches) is carried out based on the Jones formalism for vectors and matrices [1–6]. Calculation of the optical circuit involves Jones matrices for the elements included in the circuit [7]. The predominant factor in analyzing the influence of polarization mismatches of the optical circuit

elements is inaccurate mutual orientation of the elements' polarization axes of the elements, taken into account by introducing the corresponding rotation matrices [1–8].

Another problem in mismatch analysis calculating Jones matrices using the elements accounting for their real polarization properties, different from the idealized representation [9]. Even though the PM fiber is one of the key elements of fiber circuits in polarization optics, selecting the appropriate Jones matrix to describe real PM fibers is an important issue that requires separate consideration.

In the ideal case, a PM filter is a linear phase plate whose Jones matrix in the Cartesian basis of Jones vectors has the well-known form [1, 2, 10]:

$$\mathbf{M}_0 = \begin{bmatrix} e^{j\varphi/2} & 0 \\ 0 & e^{-j\varphi/2} \end{bmatrix}. \tag{1}$$

This notation corresponds to the format of a special unitary matrix, which does not take into account the overall phase shift and the polarization-independent loss coefficient. It is also assumed that the matrix is written in the basis where the *X*-axis is aligned with the fast polarization direction.

The eigenvalues of matrix (1) have the form

$$\lambda_1 = e^{j\varphi/2},\ \lambda_2 = e^{-j\varphi/2},$$

where φ is the phase difference of polarization eigenstates (polarization modes) during a pass through the plate.

The quantity φ is the only parameter of the Jones matrix of an ideal PM fiber, typically uncontrolled and considered arbitrary in the calculations. It is evident that the eigenvectors of matrix (1) have the form

$$\mathbf{J}_{01} = \begin{bmatrix} 1 \\ 0 \end{bmatrix}, \quad \mathbf{J}_{02} = \begin{bmatrix} 0 \\ 1 \end{bmatrix}. \tag{2}$$

Strictly speaking, multiplying any of vectors (2) by an arbitrary complex number also produces eigenvectors of $\mathbf{M}_0$. However, form (2) is generally accepted, these vectors are normalized and have the same zero phase. Vectors (2) correspond to linearly polarized waves with orthogonal orientation, i.e., polarization modes of an ideal PM fiber.

Real PM fibers differ from the ideal representation, and the Jones matrix, which describes the transformation of the polarization state in such fibers, differs from form (1), albeit weakly. Imperfections are caused both by internal factors arising during manufacturing of the fiber, and by weak induced anisotropy, due to bends and twists of the fiber when it is installed in the circuit. Complex irregular variations of anisotropy generally occur in both cases, differing in different segments of the fiber. Therefore, the specific resulting properties of the Jones matrix of a real segment of PM fiber are actually unpredictable and, moreover, can change if the external conditions or the position of the fiber change. Therefore, analysis of the influence of imperfections in the PM fiber on the performance of optical circuits with such waveguides should include arbitrary cases of weak deviation of matrix (1).

Notably, the polarization properties of imperfect PM fibers have been considered in the literature, especially for the case of extended paths [11–13]. Depending on the considered mechanisms behind the deviation from the ideal structure of the fiber, such analysis was typically performed with a model comprising a set of segments of ideal fibers with small random angles between the polarization axes of the segments or some model of distributed coupling between polarization modes with analysis of coupled wave equations. The resulting Jones matrix either does not have to be constructed at all for such models, or is represented by a complex structure (for example, a product of matrices for individual segments of the fiber under consideration) with a large number of random parameters. This is justified for understanding the mechanisms behind deviations from ideal linear birefringence in real optical fibers, the spatial characteristics of mode coupling in extended optical fibers, and other similar issues.

However, a relatively simple model of the Jones matrix of a real PM fiber is often convenient for analyzing polarization mismatches in circuits with relatively short PM fibers, adequately

describing the possible transformations of the polarization state by such a fiber with a minimum number of variable parameters.

We were unable to uncover any literature dealing with this type of the Jones matrix of a real PM fiber.

The goal of this study is therefore to obtain the expressions for the Jones matrix that adequately describes the real PM fiber, as well as to analyze its properties and applications.

Jones matrices for a real PM fiber

The analysis is based on the following provisions.

If the ideal PM fiber corresponds to a linear phase plate with a given direction of polarization axes and Jones matrix (1), then the real PM fiber differs from the ideal one, which should be interpreted as perturbation of ideal linear anisotropy of the fiber.

While the anisotropy may generally vary by different patterns, the fiber is assumed to remain an element with phase anisotropy described by a unitary Jones matrix in the case of weak perturbation. This condition is consistent with negligible optical losses and, accordingly, the absence of dichroism in real relatively short PM optical fibers (less than 1 km long); it is assumed that weak perturbations do not change this circumstance. For this reason, the PM fiber corresponds to the more general case of phase anisotropy that is an elliptical phase plate, but the eigenvectors must remain close to vectors (2), i.e., correspond to polarization states with ellipticity close to zero and azimuths orthogonal to each other and close to orientation along and across the *X* axis, as in the case of vectors (2).

In view of the above, the required matrix can be constructed based on the Jones matrix of an elliptical phase plate, considering the case when ellipticity is close to zero and the deviation angle of the plate axis from the X *axis* is small. However, no explicit form of the matrix of an elliptical phase plate is given in the existing literature for representation in terms of the parameters of ellipticity angle and the azimuth of its polarization eigenstates.

Therefore, it seems expedient to use a generalized representation of the 2 × 2 matrix in terms of its eigenvectors to obtain the necessary result. Generally speaking, this method allows to obtain any Jones matrix with the known properties of eigenvectors. A simple explicit form of the required Jones matrix is obtained taking into account the required properties of the eigenvectors for the considered case of a weakly perturbed linear phase plate.

In the general case, given the parameters of the polarization ellipse, namely, the azimuth Θ and the ellipticity angle ε –, the corresponding vector can be written in the following form with an accuracy up to a constant complex multiplier [2, 3]:

$$\mathbf{J}(\Theta,\varepsilon)=\begin{bmatrix}\cos\Theta\cdot\cos\varepsilon - j\sin\Theta\cdot\sin\varepsilon\\ \sin\Theta\cdot\cos\varepsilon + j\cos\Theta\cdot\sin\varepsilon\end{bmatrix}, \tag{3}$$

so that form (3) defines a normalized Jones vector with a unit length.

In the case of an ideal linear phase plate (ideal PM fiber), the polarization eigenstates have Jones vectors (2) and correspond to polarization ellipses with $\Theta_1 = 0$, $\Theta_2 = \pi/2$ and with $\varepsilon_1 = \varepsilon_2 = 0$.

If perturbation of an ideal linear phase plate is introduced, it is assumed that the eigenvectors deviate from the ideal case, for example, Θ_1 and ε_1 are nonzero. However, since a weak perturbation is considered, we assume that conditions Θ_1, $\varepsilon_1 << 1$ are satisfied. Because Θ_1 and ε_1 are small, expansion of trigonometric functions can be applied in the general form (3): the approximate equalities $\sin x \approx x$ and $\cos x \approx 1 - x^{2/2}$ are satisfied for $x << 1$. If only first-order components are preserved, we obtain the following form for the eigenvectors of the matrix of the weakly perturbed linear phase plate:

$$\mathbf{J}_1 = \begin{bmatrix}1 - j\Theta\cdot\varepsilon\\ \Theta + j\varepsilon\end{bmatrix}, \quad \mathbf{J}_2 = \begin{bmatrix}-(\Theta - j\varepsilon)\\ 1 + j\Theta\cdot\varepsilon\end{bmatrix}. \tag{4}$$

To simplify further notation, the quantities Θ_1 and ε_1 in the expression for the vector $\mathbf{J}_1$ are written without the subscript 1. The form of the vector $\mathbf{J}_2$ can be obtained formally as a vector

orthogonal to the vector $\mathbf{J}_1$, or directly by substituting the azimuth $\Theta + \pi/2$ and the ellipticity angle $-\varepsilon$ into form (3), which corresponds to the parameters of the orthogonal polarization state. Evidently, if the values of Θ and ε tend to zero, vectors (4) are transformed to (2) for an ideal linear phase plate.

The Jones matrix has the following general representation in terms of eigenvalues and eigenvectors [1, 2]:

$$\mathbf{M} = \frac{1}{\mathbf{j}_{1x}\mathbf{j}_{2y} - \mathbf{j}_{1y}\mathbf{j}_{2x}} \begin{bmatrix} \mathbf{j}_{1x}\mathbf{j}_{2y}\lambda_1 - \mathbf{j}_{2x}\mathbf{j}_{1y}\lambda_2 & -(\lambda_1 - \lambda_2)\mathbf{j}_{1x}\mathbf{j}_{2x} \\ (\lambda_1 - \lambda_2)\mathbf{j}_{1y}\mathbf{j}_{2y} & \mathbf{j}_{1x}\mathbf{j}_{2y}\lambda_2 - \mathbf{j}_{2x}\mathbf{j}_{1y}\lambda_1 \end{bmatrix}, \tag{5}$$

where $\mathbf{j}_{1x}$, $\mathbf{j}_{1y}$ are components of the Jones vector $\mathbf{J}_1$; $\mathbf{j}_{2x}$, $\mathbf{j}_{2y}$ are components of the Jones vector $\mathbf{J}_2$.

In the case of a special unitary matrix describing a lossless system, with eigenvalues $\lambda_1 = e^{j\varphi/2}$ and $\lambda_2 = e^{-j\varphi/2}$ [4], we obtain from the general form (5):

$$\mathbf{M} = \frac{1}{\mathbf{j}_{1x}\mathbf{j}_{2y} - \mathbf{j}_{1y}\mathbf{j}_{2x}} \begin{bmatrix} \mathbf{j}_{1x}\mathbf{j}_{2y}e^{j\varphi/2} - \mathbf{j}_{2x}\mathbf{j}_{1y}e^{-j\varphi/2} & -j2\mathbf{j}_{1x}\mathbf{j}_{2x}\sin(\varphi/2) \\ j2\mathbf{j}_{1y}\mathbf{j}_{2y}\sin(\varphi/2) & \mathbf{j}_{1x}\mathbf{j}_{2y}e^{-j\varphi/2} - \mathbf{j}_{2x}\mathbf{j}_{1y}e^{j\varphi/2} \end{bmatrix}. \tag{6}$$

If we substitute expressions (4) into Eq. (6), we can find the coefficients of the matrix for the case of weak perturbation of a linear phase plate. They have the form

$$\begin{aligned} m_{11} &= (1+\Theta^2\varepsilon^2)e^{j\varphi/2} + (\Theta^2+\varepsilon^2)e^{-j\varphi/2}, \\ m_{22} &= (1+\Theta^2\varepsilon^2)e^{-j\varphi/2} + (\Theta^2+\varepsilon^2)e^{j\varphi/2}, \\ m_{21} &= j2(\Theta + j\varepsilon)(1 + j\Theta\varepsilon)\sin(\varphi/2), \\ m_{12} &= j2(1 - j\Theta\varepsilon)(\Theta - j\varepsilon)\sin(\varphi/2), \\ \mathbf{j}_{1x}\mathbf{j}_{2y} - \mathbf{j}_{1y}\mathbf{j}_{2x} &= (1+\Theta^2\varepsilon^2) + (\Theta^2+\varepsilon^2) \approx 1 + \Theta^2 + \varepsilon^2. \end{aligned} \tag{7}$$

Expressions (7) are obtained based on vectors (4) that take into account only first-order smallness with respect to Θ and ε. Therefore, assuming that the conditions Θ, $\varepsilon << 1$ are strictly satisfied, it is expedient to also omit the second-order components in the coefficients of the matrices, since they have an extremely weak effect on quantitative results in the calculations. An exception would be the situation when the formulas for the coefficients of the matrix would include only high-order perturbation components, but there are no such coefficients in expressions (7). When the second-order components are excluded, matrix (7) of a weakly perturbed linear phase plate is transformed to

$$\mathbf{M}_{\text{PMF}}(\Theta, \varepsilon) = \begin{bmatrix} e^{j\varphi/2} & 2(\varepsilon + j\Theta)\sin(\varphi/2) \\ -2(\varepsilon - j\Theta)\sin(\varphi/2) & e^{-j\varphi/2} \end{bmatrix}. \tag{8}$$

The determinant Δ of matrix (8) is equal to the expression

$$\Delta = 1 + 4(\Theta^2 + \varepsilon^2)\cdot\sin^2(\varphi/2),$$

it is real, but differs from unity.

To strictly correspond to a normal unitary matrix, a multiplier $1/\Delta$ can be introduced into expression (8), but in practice it seems advisable to neglect the correction with second-order smallness with respect to Θ and ε, using instead expression (8) without additional multipliers.

To represent the ideal matrix $\mathbf{M}_0$ by taking into account small ellipticity angles and azimuths of polarization eigenstates, let us consider two special cases of matrix (8).

If either the azimuth of linear polarization eigenstate is only rotated weakly ($\varepsilon = 0$), or weak ellipticity occurs ($\Theta = 0$), then the Jones matrix (8) is transformed to the cases

$$\mathbf{M}_{\text{PMF\_}\Theta} = \begin{bmatrix} e^{j\varphi/2} & j2\Theta\cdot\sin\dfrac{\varphi}{2} \\ j2\Theta\cdot\sin\dfrac{\varphi}{2} & e^{-j\varphi/2} \end{bmatrix}, \quad \mathbf{M}_{\text{PMF\_}} = \begin{bmatrix} e^{j\varphi/2} & 2\varepsilon\cdot\sin\dfrac{\varphi}{2} \\ -2\varepsilon\cdot\sin\dfrac{\varphi}{2} & e^{-j\varphi/2} \end{bmatrix}. \tag{9}$$

These particular cases of matrices are also interesting because they can be directly compared with the expressions obtained relatively simply from the cases given in the literature. This is discussed in Appendix I considering the rotation of a linear phase plate and in Appendix II analyzing the expression for an elliptical phase plate oriented along the *X* axis.

Fig. 1,*a* additionally illustrates our analysis, showing a Poincaré sphere with an explanation of the parameters used. The points *A* and *B* correspond to polarization of the vector $\mathbf{J}_1$ for the cases of the ideal and real Jones matrix of the PM fiber.

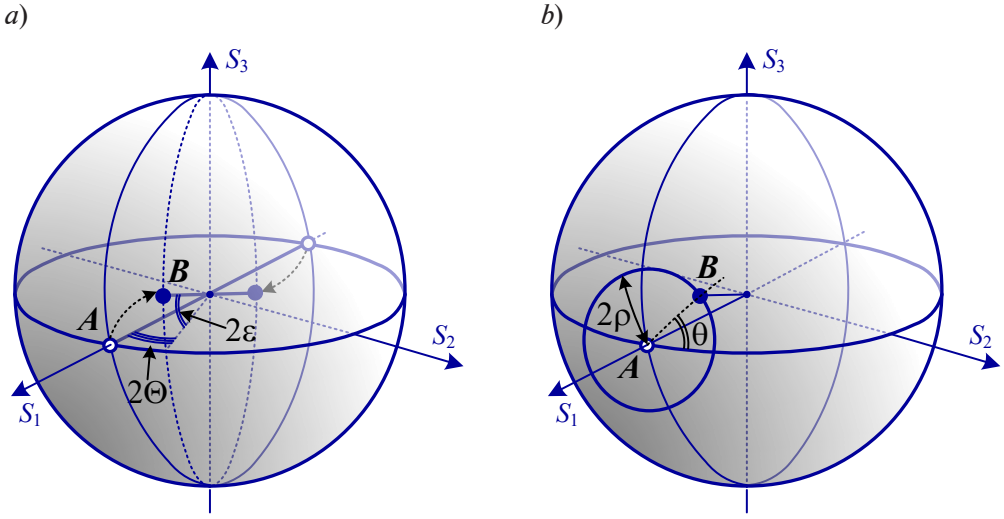

Fig. 1. Deviation of PM fiber eigenvector point
on the Poincaré sphere during perturbation of the fiber:
Θ, ε are the azimuth and ellipticity angle; 2ρ is the great-circle distance;
points *A* and *B* correspond to polarization of the vector $\mathbf{J}_1$ for the cases
of Jones matrices for ideal and real PM fiber, respectively

The Jones matrix (8) for the case of a weakly perturbed linear phase plate can be used for modeling systems with birefringent optical fibers.

The imperfection of the fiber is described by two independent parameters Θ and ε, however, there is no single parameter characterizing the deviation of the real matrix $\mathbf{M}_{\text{PMF}}$ from the ideal variant $\mathbf{M}_0$. If the values of Θ, ε, and, accordingly, eigenvectors (4) are given, an appropriate quantitative parameter characterizing perturbation is the angular distance between points on the Poincaré sphere corresponding to the ideal case with angular coordinates {0; 0} and the non-ideal one with coordinates {Θ; ε}. Indeed, the great-circle distance (also called the spherical distance), given by two points on the Poincaré sphere (the shortest distance corresponding to a great-circle arc of the sphere containing these points), best characterizes the difference in polarization states [14]. Since the Poincaré sphere has a unit radius, both the geometric and angular (in radians) great-circle distances are the same. If one point on the Poincaré sphere corresponds to zero angular coordinates, then the angular great-circle distance to a point with coordinates {Θ; ε} is given by a simple expression:

$$\cos 2\rho = \cos 2\Theta \cdot \cos 2\varepsilon,$$

where the great-circle distance is denoted as 2ρ (the coefficient 2 is introduced to simplify further formulations).

This expression corresponds to a small circle of the Poincaré sphere with the center in zero angular coordinates and a radius 2ρ (Fig. 1,*b*). Since the quantities Θ and ε are small, this relationship is reduced to a simpler expression:

$$\rho^2 = \varepsilon^2 + \Theta^2, \tag{10}$$

corresponding to the equation of a circle on the plane.

Note that the imposed conditions Θ, ε << 1 also assume that the condition ρ<< 1 is satisfied.

The parameter ρ also gives a unified quantitative characteristic for the level of deviation of the PM fiber from the ideal case for the matrix with the selected values of Θ and ε. The maximum potential deviation ρ_{max} of the real PM fiber from the idealized representation can be given in analysis and calculations, and then the parameters ε and Θ should clearly be considered under the constraint

$$(\varepsilon^2 + \Theta^2) \le \rho_{max}{}^2.$$

It may be more convenient to analyze and model real PM fibers based on a different logic for constructing the fiber matrix, selecting the initial value of ρ. It is inconvenient to use the relationship of Θ and ε with the parameter ρ based on expression (10), especially since it is ambiguous. However , this expression corresponds to the equation of a circle with the radius ρ, and it is convenient to determine the position of a point on a circle with a given radius by some angle θ. If it is counted from the direction along the equator of the Poincaré sphere, as shown in Fig. 1,*b*, i.e., assuming that θ = 0 at Θ = ρ and ε = 0, then the parameters Θ and ε are given by simple expressions:

$$\Theta(\rho,\theta) = \rho \cdot \cos\theta;\ \varepsilon(\rho,\theta) = \rho \cdot \sin\theta. \tag{11}$$

Thus, the given value of ρ determines the level of small deviation of the polarization eigenstate of the perturbed linear phase plate, which is supplemented by the option to select the specific type of perturbation due to arbitrary choice of the angular parameter θ. Then, taking into account expressions (8) and (11), the matrix of the perturbed linear phase plate can be written with the given parameter of perturbation smallness ρ and the argument θ in the form

$$\mathbf{M}_{\text{PMF}}(\rho,\theta) = \begin{bmatrix} e^{j\varphi/2} & j2\rho \cdot e^{-j\theta}\sin(\varphi/2) \\ j2\rho \cdot e^{j\theta}\sin(\varphi/2) & e^{-j\varphi/2} \end{bmatrix}. \tag{12}$$

This case of Jones matrix of a real PM fiber, as well as form (8), has two variable parameters accounting for imperfection of the fiber. However, it may be more convenient to use the parameters ρ and θ, offering advantages in calculations with varying parameters, which is discussed below.

Application of obtained Jones matrices of real PM fiber to analysis and numerical modeling of circuits

The analysis carried out concerned several aspects important for calculations on the influence of imperfections in PM fibers and other polarizing fiber-optic elements (referred to as polarization mismatches of the elements) on the operation of the circuits containing them.

The parameters of the Jones matrix characterizing deviation from its ideal form, which must be varied to consider all of their possible values that cannot be predicted in advance, are not the only factor influencing the calculations of signal distortions in fiber-optic circuits with polarizing elements. The phase difference φ also affects the distortion of the signal generated in the circuit compared to the ideal and matched polarizing elements; the difference φ should also be varied in the interval 2π during the analysis. Consequently, a range of parameters have to be varied in circuits with even a small number of fiber-optic polarizing elements and PM fibers to study the effect of polarization mismatches, so that the worst possible types of distortions in the circuit's operation can be identified. Therefore, comprehensive analysis of polarization mismatches in circuit elements generally requires numerical calculations by computing means, and the computational costs for iterative calculations over a large number of parameter values may be high.

Numerical computations of the Jones matrix for a real PM fiber assuming certain deviation parameters of the eigenvectors given by the values of Θ and ε, can be performed by directly using the general structure of the Jones matrix (6). The form (II-6) can be used (see Appendix II) for eigenvectors (the first one corresponds to vector (3), the second one is orthogonal to the first one), followed by calculating the matrix (6). The form of the general matrix of an elliptical phase plate given in Appendix II can also be used. Expressions (II-7) are obtained precisely by substituting (II-6) into form (6), but take into account some simplifications based on trigonometric identities. The case based on such general structures has an advantage, since they are correct even if the condition smallness is not sufficiently satisfied for Θ or ε and the distortion level ρ introduced cannot be considered sufficiently low. However, the obtained matrices (8) and (12) are much simpler and do not include trigonometric functions with respect to variable parameters. This not only makes it possible to obtain analytical results for distortions of the resulting signals in the analyzed circuits in some cases, but also significantly reduce computational costs in numerical calculations.

Another aspect is related to organizing calculations with a varying a set of parameters. In practice, this implies searching through the values of all these parameters, calculating some resulting circuit signal for each specific combination of values. The possible maximum distortion level of the eigenvectors in the element's Jones matrix should be assessed based on empirical data or the results of additional theoretical studies of perturbation of a particular fiber element. The ρ_{max} parameter mentioned above serves for this purpose in the case of PM fiber. An alternative logic is possible when calculation and analysis involves searching for the maximum permissible peturbation level ρ_{max}, which must be provided for an acceptable distortion level of the circuit signals. In any case, analysis based on the generalized structures of the fiber's Jones matrix or based on matrix (8) has to involve a search through two variable parameters Θ and ε in the variation ranges from $-\rho_{max}$ to ρ_{max}, satisfying the condition

$$\Theta^2 + \varepsilon^2 \le \rho_{max}{}^2.$$

Generally speaking, it is not quite convenient to vary two independent parameters in the same common range, but with a dependent boundary of one parameter at a specific value of the second one. It seems more convenient and expedient to organize the search through variable parameters using matrix (12) with ρ and θ replacing the parameters Θ and ε. If form (12) is used, the quantity ρ should be varied independently in the range from $-\rho_{max}$ to ρ_{max}, and θ in the range from 0 to 2π.

There is another aspect related to analysis of polarization mismatches in circuits with PM fibers and the matrices considered. As already noted, such analysis often starts with considering only the angular misalignment between the polarization axes of PM fibers in splices or connectors joining the polarization splitters [7, 8]. On the one hand, this approach is adopted because it is very simple to account for such a misalignment within the framework of the Jones matrix formalism. The coupling is taken into account by introducing a rotation matrix [2, 3]:

$$\mathbf{R}(\alpha) = \begin{bmatrix} \cos\alpha & \sin\alpha \\ -\sin\alpha & \cos\alpha \end{bmatrix}, \tag{13}$$

where α is the angle between the directions of the polarization axes of connected fibers.

The angle α in the calculations should be varied in the range $[-\alpha_{max}, \alpha_{max}]$, taking into account the estimated level of possible angular misalignment.

On the other hand, this approach implies that the influence of angular misalignment between the polarization axes of coupled PM fibers can be greather than that of the imperfections of individual fibers.

The angular alignment of the axes in modern PM fiber splices is no worse than 3–5°, which corresponds to the typical extinction rates for connectors of PM fibers in the range of 20–25 dB [15, 16]. However, special splicers make it possible to achieve the alighnment up to up to 1° in polarization axes of PM fibers in fusion splicings. However, perturbations of even short PM fibers can also have ρ values of order of 1°, as confirmed by our experimental findings (see below).

Thus, in practice, the level of angular misalignment of PM fibers connected can be comparable to the mismatch level ρ_{max} associated with the imperfection of the PM fibers. In fact, accounting

for the imperfection of PM fiber in the calculations only makes sense when its ρ_{max} level is comparable or higher than the misalignment level of the angles between the polarization axes α_{max}.

In cases where $\rho_{max} \approx \alpha_{max}$ or $\rho_{max} > \alpha_{max}$, it turns out that the Jones matrix of a real PM fiber already takes into account the possible azimuth shift of its polarization eigenstate, including the azimuth shift at zero ellipticity angle, which describes a particular case of angular misalignment only. Then adopting the approach described above makes it possible to exclude specifically accounting for the angles α and the corresponding rotation matrices in the calculations (see Fig. 2). If PM fibers are represented by an ideal model with a matrix of the form $\mathbf{M}_0$ (this is shown in Fig. 2,*a*), taking into account two connected fibers in the calculations implies that they are described by the matrix

$$\mathbf{M}_{0(i+1)} \cdot \mathbf{R}(\alpha) \cdot \mathbf{M}_{0i},$$

where i, $i + 1$ are the numbers of the connected fibers in the direction of light propagation.

However, if one of the PM fibers or both are described by a model with the matrix $\mathbf{M}_{PMF}$, then potential angular misalignments are already taken into account in the calculations by the parameter Θ. Then, the following matrices can be used in the calculations:

$$\mathbf{M}_{0(i+1)} \cdot \mathbf{M}_{PMFi} \text{ or } \mathbf{M}_{PMF(i+1)} \cdot \mathbf{M}_{PMFi} \text{ or } \mathbf{M}_{PMF(i+1)} \cdot \mathbf{M}_{0i},$$

depending on which fibers are described by the imperfect fiber model.

Thus, the given properties of the matrix $\mathbf{M}_{PMF}$ allow to exclude the rotation matrices from the description of circuits with PM fibers to account for angular misalignment in fiber connections, which can considerably simplify the calculations by reducing the number of variable parameters.

Moreover, this approach provides a certain unification of the circuit model, because even if it is angular misalignments that are predominant, it can be assumed that $\varepsilon = 0$ in the matrix $\mathbf{M}_{PMF}$ of the form (8). On the other hand, using matrices $\mathbf{M}_{PMF}$ does not always allow to completely exclude rotation matrices from the description of PM fiber connections. This point is illustrated in Fig. 2,*c*, where a real PM fiber is connected at both ends to fibers or other polarization elements, which are described by ideal matrices with a strictly defined axis orientation. In this case, the angle Θ in the matrix $\mathbf{M}_{PMF}$ takes into account the same shift in the axis orientation at both ends of the fiber, even though the angular mismatch due to inaccurate orientation of the fibers at the connections may be different at different ends of the fiber. Therefore, a rotation matrix should be introduced at one end of the fiber for correct description. This means that caution should be exercised in excluding the rotation matrices from the description of connections so as not to miss those cases of angular misalignment that are not taken into account in the matrices $\mathbf{M}_{PMF}$.

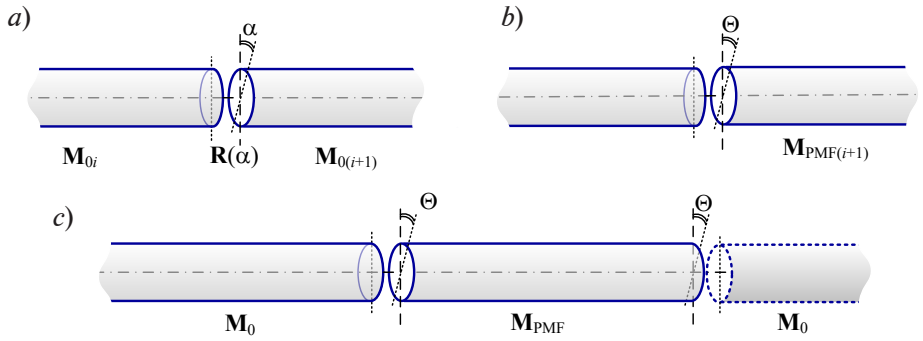

Fig. 2. Examples of accounting for orientation mismatches of polarization axes in connected optical fibers (see explanations in the text)

Experimental

This section describes experiments aimed at studying the properties of real PM fibers and their differences from an idealized linear phase plate; an approximate estimate was obtained for the the parameter ρ introduced earlier for real fibers.

One of the best-known theoretically and experimentally studied phenomena illustrating the imperfections in PM fibers is the coupling of polarization modes [11, 13]. For example, such

imperfection appears when one linearly polarized eigenmode is excited at the input and when both this and orthogonal polarization modes are detected at the output. However, it is difficult to unambiguously interpret the formation of a spurious mode at the fiber output and its relative level in the context of the Jones matrix of PM fiber discussed above. This is especially true for modeling within the framework of the Jones matrix formalism of complex fiber-optic circuits including PM fibers.

Apparently, the most acceptable approach to determining the parameters of imperfections in PM fibers is based on measurements allowing to find the Jones matrix of an element by measuring the output polarization state at different input polarization states appear. For example, linearly polarized light with orientations of 0, 45 and 90° relative to an arbitrarily selected *X* axis can be used at the fiber input, to subsequently calculate the Jones matrix of the fiber using the measured parameters of the polarization state at the fiber output by the formulas given in [6, 17].

However, in this study we consider very slight deviations of the parameters Θ and ε of the Jones matrix from zero (about 1° or even smaller). This means that the accuracy with which linear polarization of light is oriented at the fiber input must be significantly better, while ellipticity should be much smaller, which is difficult to achieve in normal laboratory conditions with standard devices.

In view of these obstacles, we chose another measurement setup to approximately extimate the level of ρ values in real PM fibers (see the scheme in Fig. 3). The fiber tested is excited by laser radiation during measurements, some segment of the fiber is heated, and a polarimeter records the heating-induced evolution of the polarization state at the fiber output.

Consider the following well-known circumstances to understnad the principle underlying the experiments carried out. As light passes through an element with phase anisotropy, for example an optical fiber, the polarization state undergoes specific transformations. The crucial aspect here is that this transformation corresponds to rotation of the surface of the Poincaré sphere around an axis given by the polarization eigenstates of the element by an angle corresponding to the difference in phase delays φ of these states [1, 6, 13]. If the phase difference φ varies monotonically in the range above 2π, then the evolution of the output polarization state on the Poincaré sphere is a small circle of the sphere whose angular radius *R* is determined by the ratio of amplitudes of polarization modes [1, 6, 18]. The variation in φ in the scheme shown in Fig. 3,*a* is induced by heating of a fiber segment; the polarimeter records the resulting evolution of the polarization state of light. Next, the measured values of the polarization state (points on the Poincaré sphere) can be approximated by a circle to determine its parameters, namely the radius *R* and the angular coordinates of the circle center $2\Theta_0$ and $2\varepsilon_0$. Since the circle center corresponds to the point of the polarization eigenstate of the fiber, the coordinates of the center Θ_0 and ε_0 represent the required parameters of the matrix $\mathbf{M}_{\text{PMF}}$ of the fiber tested. Fig. 3,*b* shows the Poincaré sphere with the point *B* corresponding to the polarization eigenstate of the fiber considered (as in Fig. 1).

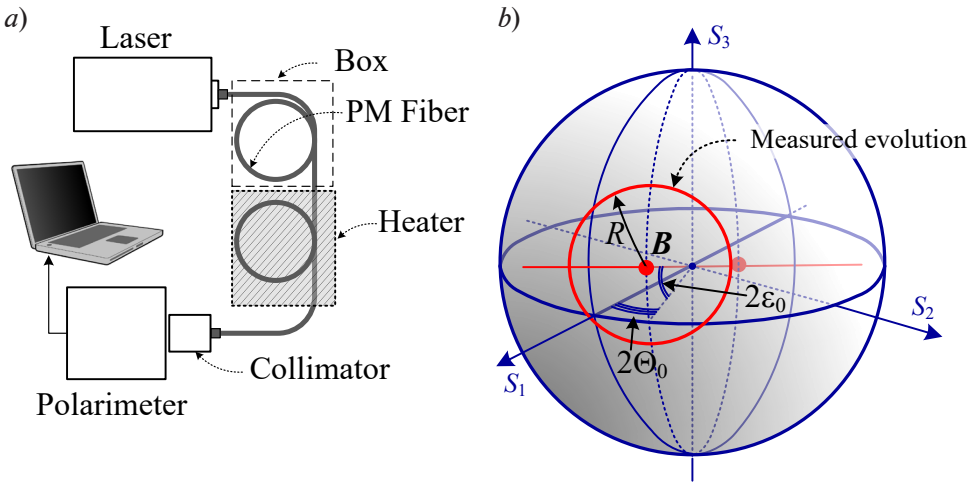

Fig. 3. Experimental setup (*a*) and evolution of polarization state on the Poincaré sphere, recorded during the measurements (*b*)

We previously carried out such measurements to detect the level of spurious mode at the output of PM fibers by the found value of *R*. However, approximating the measured points on the Poincaré sphere by a circle allows to determine not only *R*, but also the center of the circle *B*, i.e., the values of Θ_0 and ε_0. Any specific polarization states do not have to be determined precisely at the output of the fiber in this case.

Admittedly, there are some peculiarities stemming from the above-described main principle behind the transformation of the polarization state of light propagating through the fiber.

Firstly, the position of the center of the observed circle on the Poincaré sphere does not depend on the properties of the initial fiber segment up to the section that is heated. If the polarization properties of this segment are static, then it can determine the polarization state of light at the input to the heated section and, accordingly, affect *R*, but not the position of point *B*.

Secondly, heating can transform the polarization eigenstates in real fibers, due to irregular mechanisms governing the distortion of PM fiber properties. However, in this case, the circular evolution of the polarization state at the output is distorted, forming spirals and other shapes deviating from the circle.

Thirdly, the position of the recorded point *B* can depend not only on the eigenmodes of the heated fiber section, but also on the eigenmodes of the fiber section between the heater and the polarimeter. The propagation of radiation through this segment can also rotate the surface of the Poincaré sphere (together with the circular evolution produced at the output from the heated section) around the axis already given by the modes of the output segment. However, this circumstance affects the result only if the eigenmodes of the heated and output segments differ; this, however, does not prevent us from recording the very fact of deviation of the measured point *B* from the point {0; 0} corresponding to the ideal PM fiber.

A highly coherent RIO-Orion laser (Redfern Integrated Optics, USA) with an FC/APC connector was used in the measurements to connect the PM fiber and excite mainly one linear polarization mode (according to the laser's specifications, the extinction rate exceeds 20 dB).

The experimental conditions created provided relatively low values of *R*, illustrating the deviations of the center of the observed circle on the Poincaré sphere more clearly. The laser's output power in the fiber was 10 MW. The polarization state was measured with a PAX1000IR2 polarimeter (Thorlabs, USA). This device measures the azimuth and ellipticity angle of the polarization state with an accuracy of 0.25°. The fiber patch cord was connected to the polarimeter by a collimator with a ferrule connector (FC) installed at the input to the polarimeter. The connector keying position was oriented approximately relative to the polarimeter axis and remained unchanged during the experiments.

The first stage of measurements consisted of testing three PM patch cords with a length of 1 m, terminated by FC/APC connectors. Patch cord samples 1 and 2 were purchased from AFW Technologies (Australia, model PMP-15-R-L-1), and patch cord 3 was included with the laser source. The output section of the fiber patch cord (about 20 cm long) was heated to 70 °C for 20 minutes, which was sufficient to change the phase difference φ of polarization eigenmodes by about 2π.

The results of the measurements are shown in Fig. 4 and in Table 1. Since the rotation of the collimator relative to the polarimeter axis was set manually and the direction of the fiber axis only approximately corresponded to the polarimeter axis, it is not the measured values of Θ_0 that are informative but rather their difference for different patch cords.

The results indicate that the observed evolution of the polarization state at the output from the PM fiber patch cord is in excellent agreement with the circumference. At the same time, there is a significant difference in *R* values for different patch cords, which is most likely due to a mismatch in the orientation of polarization axes of PM fibers connected with the laser.

Notably, the parameter *R* is introduced as the angular radius of the small circle on the Poincaré sphere, when the angular coordinates are determined by the doubled angles Θ and ε. A circle with half the radius is obtained if points on the plane are plotted in coordinates Θ and ε without doubling (Fig. 4,*b*). The values of the azimuth Θ_0 for the patch cords differ by about 3.5°, and there is also a non-zero ellipticity angle ε_0, which diverges for different patch cords in a range exceeding 1.5° (from -1.09° to 0.63°). The spread in Θ_0 values may not be caused by internal inhomogeneities of the fiber but to rotation of the fiber when it is connected to the collimator if the keying is attached inaccurately. However, the difference in the values of the ellipticity angle exceeding 1.5° indicates a difference in the polarization eigenstates of fiber patch cords.

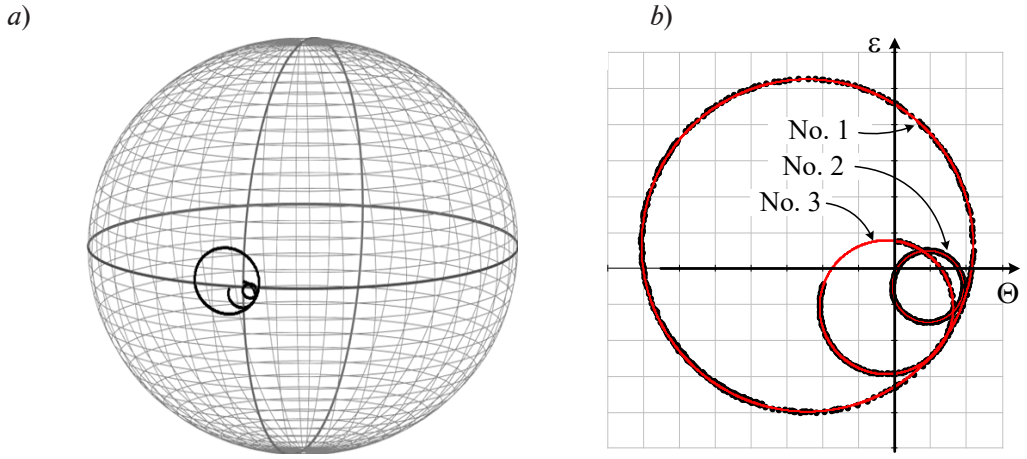

Fig. 4. Evolution of polarization state on the Poincaré sphere (*a*) and on the plane, in the coordinates Θ and ε (*b*). No. 1, No. 2, No. 3 are patch cord numbers. The scale unit is 1 degree. Approximation of experimental points by a circle on the Poincaré sphere is shown by red lines

Table 1

Parameters of circles approximating the measured points of evolution in polarization state on the Poincaré sphere. First stage of experiment (see Fig. 4)

Angular parameter	Parameter value, degrees, for patch cord		
	No. 1	No. 2	No. 3
Radius R	9.24	1.99	3.72
Azimuth Θ_0	–2.44	0.92	–0.24
Ellipticity ε_0	0.63	–0.51	–1.09

A segment of HB1250 PM fiber from Fibercore (USA), slightly longer (200 m) compared to the length of the patch cords, was considered at the second stage of the experiments. The laser excited mainly one polarization mode in the fiber. The entire path was heated to 40 °C, and then the evolution of the polarization state at its output was recorded as the fiber cooled down to about 25 °C. In this case, the fiber segments in front of the heater and behind it were relatively short, and the temperature varied in the most part of the fiber.

At this stage of the experiment, transformations in the polarization properties were clearly manifested as variation in the level of spurious polarization mode at the output, which can be interpreted as interference from the components of this mode migrating from the main mode in different segments of the fiber with different phase delays that vary with temperature. The change in the level of spurious mode corresponds to the change in the radius R of the recorded circular trajectory on the Poincaré sphere. On the other hand, this means that a change in the temperature of such a long fiber can transform its polarization eigenstates in the presence of complex birefringence inhomogeneities in the fiber. Therefore, a change in the radius R should also be accompanied by changes in the center of the circle formed on the Poincaré sphere.

The evolution of the polarization state observed in this experiment is shown in Fig. 5. It is a quasi-circular motion with a changing radius, which reflects the above-described circumstances. In the context of the main issue considered in this paper, it is more important to change not the radius, but the center of the circular segments of this trajectory. Indeed, if we choose relatively small segments of the evolution in the polarization state, in general, they accurately correspond to a circle (the variation in the radius R occurs slower than the increase in the phase difference

between the modes by 2π). We can therefore assume that the centers of such circles characterize their polarization eigenstates at the appropriate moment for a given temperature. Fig. 5 shows the measured evolution of the polarization state, including examples for four fragments of the measured trajectory corresponding to temperatures of approximately 33, 30, 28 and 25 °C. These fragments were selected from a vast range of experimental data to show examples of circles with different values of parameters Θ_0 and ε_0.

Approximation of all measured points by a small circle on the Poincaré sphere gives the following parameter values, in degrees:

$$R = 7.59,\ \Theta_0 = 0.98,\ \varepsilon_0 = 0.37$$

(such a circle is shown in Fig. 5,*b* in Θ and ε coordinates). The parameters of the circles inscribed in the points of the fragments shown in Fig. 5,*d* are given in Table 2.

Because the temperature varied unevenly, the number of points on the circles differs; in fact, reciprocating motion along the trajectory on the Poincaré sphere is observed in some segments.

It follows from these results that the azimuth of polarization eigenmodes of the tested fiber varies in the range of 0.20° and the ellipticity angle in the range of 0.85°. Since measurements were carried out for a single fiber, without changing the connection to the source and the polarimeter, it is clear that the observed changes in both the azimuth Θ_0 and the ellipticity angle ε_0 point to transformation in polarization eigenstates of the fiber.

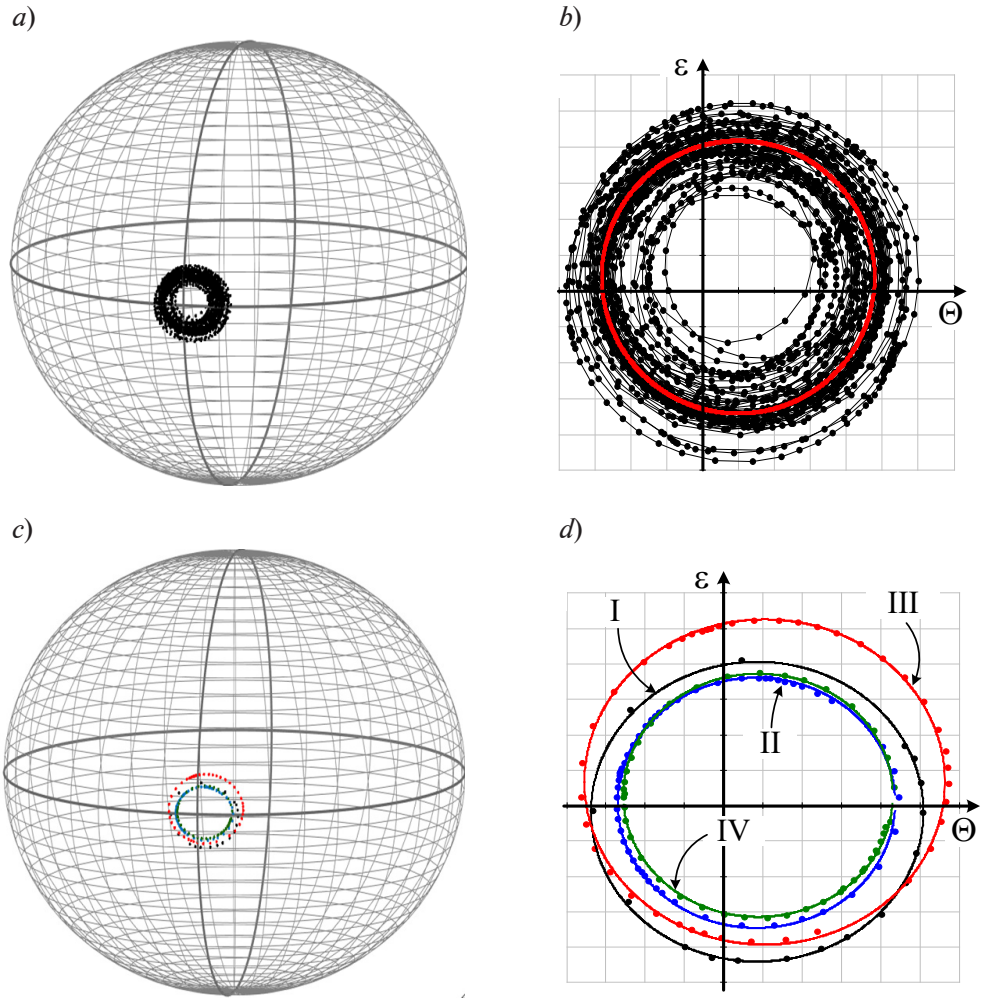

Fig. 5. Evolution of polarization state on the Poincaré sphere (*a*,*c*) and on the plane, in the coordinates Θ and ε (*b*,*d*). The cases of complete evolution (*a*,*b*) and its fragments I, II, III, IV (*c*, *d*) are shown. The scale unit is 1 degree. Approximation of experimental points by circles on the Poincaré sphere is shown by solid lines

Table 2

Parameters of circles approximating the measured points of evolution in polarization state on the Poincaré sphere. Second stage of experiment (see Fig. 5)

Angular parameter	Parameter value, degrees, for fragment			
	I	II	III	IV
Radius R	8.48	7.07	9.19	6.87
Azimuth Θ_0	0.86	0.82	1.03	0.87
Ellipticity $\varepsilon_.$	–0.18	0.07	0.66	0.28

In general, these experimental results can only be considered illustrative, as they give very approximate estimates for the degree of perturbation of the ρJones matrix in the tested fibers. Since the absolute values of the parameters Θ_0 and ε_0 cannot be regarded as completely reliable (especially those for the azimuth Θ_0), keeping in mind the errors of the polarimeter and the approximate positioning of the collimator's connector axis relative to the polarimeter axis, we did not recalculate the pairs of values $\{\Theta_0, \varepsilon_0\}$ into the value of ρ, that could be found using expression (10). However, the changes in $\{\Theta_0, \varepsilon_0\}$ can serve for approximately estimating the value of ρ at about 1°.

In addition to relative accuracy of the polarimeter readings, which is 0.25°, other error factors may affect the measurement results, for example, deviation of experimental points from the circle inscribed in them, as well as others not discussed in this study. Thus, the observed values of ρ at the level of up to 1° should be interpreted as an upper-bound estimate. However, as already noted, other key parameters, primarily angular misalignments of connected fiber axes may have the same level of values in modern circuits with fusion-spliced PM fibers.

We can therefore confirm that the conditions for small deviation of polarization properties of real PM fibers from the properties of an ideal linear phase plate are satisfied, so it is reasonable to use the Jones matrices introduced in this paper for modeling polarization mismatches in circuits with PM fibers.

Conclusion

We obtained an expression for the Jones matrix of a real PM fiber within the framework of the phase anisotropy model, accounting for weak values of ellipticity and azimuthal deviations of eigenmodes. The constructed matrix can be used to describe optical circuits with PM fibers adopting the Jones formalism to analyze the effect of polarization mismatches on the operation of the circuit. An alternative form of the Jones matrix of PM fiber is also given, where the azimuth and the ellipticity angle of the eigenstate are replaced by other angular parameters: the deviation level of the point characterizing the polarization eigenstate on the Poincaré sphere and the deviation direction of this point from the point for the ideal case. The second form of the matrix may have an advantage in modeling systems with numerical calculations and varying the imperfection parameters of PM fiber.

The experimental results illustrate the imperfections of real PM fibers, manifesting as weak variation in the ellipticity angle and azimuth of polarization modes. Furthermore, the experiments allowed to approximately estimate the level of these variations with a range of about 1°. This justifies the condition for small deviation of the ellipticity angle and azimuth imposed in the theoretical analysis for the polarization modes of PM fiber relative to the ideal model, additionally confirming that the obtained matrices can be used in analysis of modern fiber-optic circuits.

Moreover, useful expressions were constructed (see Appendix II, Eq. (II-7) below) to represent the matrix of an elliptical phase plate explicitly in terms of arbitrary ellipticity angle and azimuth of the polarization eigenstates. We have not found such an explicit form of the matrix for an arbitrary elliptical phase plate in the available literature.

Appendix I

Linear phase plate with rotation

The case when the perturbation of a linear phase plate is reduced to rotation of the directions of the polarization eigenstates, while they remain linear, can be described relatively simply. If an element with matrix (1) is rotated by an angle Θ, then its Jones matrix is determined by the following relation [2, 4–6, 10]:

$$\mathbf{M}_{\mathrm{LPP\_}\Theta} = \mathbf{R}(-\Theta)\cdot\mathbf{M}_0\cdot\mathbf{R}(\Theta)\,, \tag{I-1}$$

where the matrix **R** corresponds to rotation matrix (13). By substituting expressions (1) and (13) into relation (I-1), we obtain a matrix of a linear phase plate with the fast axis oriented at an angle Θ to the *X* axis, taking the form

$$\mathbf{M}_{\mathrm{LPP\_}\Theta} = \begin{bmatrix} \cos(\varphi/2) + j\cos 2\Theta\cdot\sin(\varphi/2) & j\sin 2\Theta\cdot\sin(\varphi/2) \\ j\sin 2\Theta\cdot\sin(\varphi/2) & \cos(\varphi/2) - j\cos 2\Theta\cdot\sin(\varphi/2) \end{bmatrix}. \tag{I-2}$$

Matrix (I-2) is valid for any angles Θ.

If we assume that the rotation angle is small, i.e., $\Theta << 1$, then the form of matrix (I-2) can be used to obtained a matrix of the form

$$\mathbf{M}_{\mathrm{LPP\_}\Theta} = \begin{bmatrix} e^{j\varphi/2} - j2\Theta^2\sin(\varphi/2) & j2\Theta\sin(\varphi/2) \\ j2\Theta\sin(\varphi/2) & e^{-j\varphi/2} + j2\Theta^2\sin(\varphi/2) \end{bmatrix}. \tag{I-3}$$

Further, if we leave only the first-order components in Θ, then matrix (I-3) is transformed to

$$\mathbf{M}_{\mathrm{LPP\_}\Theta} = \begin{bmatrix} e^{j\varphi/2} & j2\Theta\sin(\varphi/2) \\ j2\Theta\sin(\varphi/2) & e^{-j\varphi/2} \end{bmatrix}. \tag{I-4}$$

Evidently, the form of matrix (I-4) coincides with the form of Jones matrix (9).

Appendix II

Elliptical phase plate

The matrix of an elliptical phase plate is explicitly given in [2, 18] for the case when the azimuth of the polarization eigenstate (fast mode) coincides with the *X*-axis. This matrix takes the form

$$\mathbf{M}_{\mathrm{EPP}}\big|_{\Theta=0} = \begin{bmatrix} \cos(\varphi/2) + j\sin(\varphi/2)\cos 2\varepsilon & \sin(\varphi/2)\sin 2\varepsilon \\ -\sin(\varphi/2)\sin 2\varepsilon & \cos(\varphi/2) - j\sin(\varphi/2)\cos 2\varepsilon \end{bmatrix}. \tag{II-1}$$

It is easy to formulate expression (II-1) by synthesizing the Jones matrix based on structure (6). Indeed, the eigenvectors for the matrix $\mathrm{M}_{\mathrm{EPP}}|_{=0}$ are obtained by assuming that $\Theta = 0$ in the Jones vector (3), which gives the expressions

$$\mathbf{J}_1 = \begin{bmatrix} \cos\varepsilon \\ j\sin\varepsilon \end{bmatrix},\ \mathbf{J}_2 = \begin{bmatrix} j\sin\varepsilon \\ \cos\varepsilon \end{bmatrix}. \tag{II-2}$$

Substituting these expressions into structure (6) yields a matrix of the form (II-1).

If we assume that the ellipticity of the polarization eigenstates is small and $\varepsilon << 1$, then replacing the trigonometric functions in expression (II-1) with their approximate analogues, i.e., $\sin(x) \approx x$ and $\cos(x) \approx 1 - x^2/2$, we obtain a matrix of the form

$$\mathbf{M}_{\text{EPP}}\big|_{\Theta=0} = \begin{bmatrix} e^{j\varphi/2} - j2\varepsilon^2 \sin(\varphi/2) & 2\varepsilon \cdot \sin(\varphi/2) \\ -2\varepsilon \cdot \sin(\varphi/2) & e^{-j\varphi/2} + j2\varepsilon^2 \sin(\varphi/2) \end{bmatrix}. \quad \text{(II-3)}$$

If we preserve only the first-order components with respect to ε, we obtain the following expression:

$$\mathbf{M}_{\text{EPP}}\big|_{\Theta=0} = \begin{bmatrix} e^{j\varphi/2} & 2\varepsilon \cdot \sin(\varphi/2) \\ -2\varepsilon \cdot \sin(\varphi/2) & e^{-j\varphi/2} \end{bmatrix}. \quad \text{(II-4)}$$

Apparently, this result (II-4) completely coincides with the form of the Jones matrix (9).

It is logical to supplement the particular case of the matrix for an elliptical phase plate $\mathbf{M}_{\text{EPP}}|_{\Theta=0}$ with the case of the Jones matrix for an elliptical plate of arbitrary orientation.

The general form of such a matrix can be obtained based on the expression

$$\mathbf{M}_{\text{EPP}} = \mathbf{R}(-\Theta) \cdot \mathbf{M}_{\text{EPP}}\big|_{\Theta=0} \cdot \mathbf{R}(\Theta) \, . \quad \text{(II-5)}$$

However, it is possible to use a more general principle to obtain the matrix of an elliptic phase plate, applying expressions (6). Adopting the notation of the normalized Jones vector (3) and its orthogonal vector, we obtain the form of the eigenvectors of the matrix $\mathbf{M}_{\text{EPP}}$ in the general case as

$$\mathbf{J}_1 = \begin{bmatrix} \cos\Theta \cdot \cos\varepsilon - j \sin\Theta \cdot \sin\varepsilon \\ \sin\Theta \cdot \cos\varepsilon + j \cos\Theta \cdot \sin\varepsilon \end{bmatrix}, \; \mathbf{J}_2 = \begin{bmatrix} -\sin\Theta \cdot \cos\varepsilon + j \cos\Theta \cdot \sin\varepsilon \\ \cos\Theta \cdot \cos\varepsilon + j \sin\Theta \cdot \sin\varepsilon \end{bmatrix}. \quad \text{(II-6)}$$

Substituting expressions (II-6) into Eq. (6) and performing trigonometric transformations, we obtain the following general structure for the Jones matrix of an elliptical phase plate:

$$\mathbf{M}_{\text{EPP}} = \begin{bmatrix} \cos\dfrac{\varphi}{2} + j \cos 2\Theta \cdot \cos 2\varepsilon \cdot \sin\dfrac{\varphi}{2} & \left(\sin 2\varepsilon + j \sin 2\Theta \cdot \cos 2\varepsilon\right) \sin\dfrac{\varphi}{2} \\ -\left(\sin 2\varepsilon - j \sin 2\Theta \cdot \cos 2\varepsilon\right) \sin\dfrac{\varphi}{2} & \cos\dfrac{\varphi}{2} - j \cos 2\Theta \cdot \cos 2\varepsilon \cdot \sin\dfrac{\varphi}{2} \end{bmatrix}. \quad \text{(II-7)}$$

As far as we are aware, this important expression for the general case of an elliptical phase plate is absent in the literature, and can be useful for formulating Jones matrices for various particular cases of phase plates and anisotropic fibers.

REFERENCES

1. **Huard S.,** Polarization of light, John Wiley & Sons, Inc., Chichester, UK, 1997.

2. **Ishchenko E. F., Sokolov A. L.,** Polyarizatsionnaya optika [Polarization optics], Third Ed., Fizmatlit Publishing, Moscow, 2019 (in Russian).

3. **Azzam R. M. A., Bashara N. M.,** Ellipsometry and polarized light, Third ed., North Holland Publishing Company, Amsterdam, Netherlands, 1999.

4. **Gerrard A., Burch J. M.,** Introduction to matrix methods in optics, revised ed., Dover Publications, Inc., Dover, USA, 2012.

5. **Yariv A., Yeh P.,** Optical waves in crystals: propagation and control of laser radiation, John Wiley & Sons, Inc., New York, Chichester, Brislane, Toronto, Singapore, 1984.

6. **Collett E.,** Polarized light in fiber optics, SPIE Press, Bellingham, Washington, USA, 2003.

7. **Temkina V., Medvedev A., Mayzel A.,** Research on the methods and algorithms improving the measurements precision and market competitive advantages of fiber optic current sensors, Sensors. 20 (21) (2020) 5995.

8. **Krylov G. M., Fat'yanov O. V., Duplinskii A. V.,** Influence of birefringent fibre joints on the visibility drift in a Mach – Zehnder interferometer, Quantum Electron. 50 (5) (2020) 447–453.

9. **Temkina V., Medvedev A., Mayzel A., Sivolenko E.,** Quarter wave plate for fiber optic current sensor: Comparison of modeling and experimental study, In book: International Youth Conference on Electronics, Telecommunications and Information Technologies (Proc. YETI 2021, St. Petersburg, Russia), Ed. by E. Velichko, V. Kapralova, P. Karaseov, et al., Book Series "Springer Proceedings in Physics". Vol. 268. Springer Cham, 13 January (2022) 437–448.

10. **Molchanov V. Ya., Skrotskii G. V.,** Matrix method for the calculation of the polarization eigenstates of anisotropic optical resonators, Sov. J. Quantum Electron. 1 (4) (1972) 315–330.

11. **Yang J., Yu Z., Yuan L.,** Characterization of distributed polarization-mode coupling for fiber coils, In book: Peng G. D. (Ed.). Handbook of Optical Fibers. Springer Nature Singapore Pte. Ltd., Singapore, 16 May 2018.

12. **Wuilpart M., Megret P., Blondel M., et al.,** Measurement of the spatial distribution of birefringence in optical fibers, IEEE Photon. Technol. Lett. 13 (8) (2001) 836–838.

13. **Rashleigh S.,** Origins and control of polarization effects in single-mode fibers, J. Light. Technol. 1 (2) (1983) 312–331.

14. **Kells L. M., Kern W. F., Bland J. R.,** Plane and spherical trigonometry, Andesite Press, Warsaw, 2017.

15. Polarization Maintaining (PM) Patch Cord 980, 1030, 1064, 1310, 1550 nm. https://www.afwtechnologies.com.au/pm_patchcord.html. (Accessed July 27, 2023).

16. 1550 nm Polarization Maintaining (PM) Patch-cord, https://www.dkphotonics.com/product/1550nm-polarization-maintaining-patch-cord.html (Accessed July 27, 2023).

17. **Fedotov A., Ustimchik V., Rissanen J., et al.,** Active tapered double-clad fiber with low birefringence: supplement, Opt. Express. 29 (11) (2021) 16506–16519.

18. **Tentori D., Garcia-Weidner A., Kuzin E.,** On the birefringence evaluation of single-mode fibers, Rev. Mex. Fis. 62 (4) (2016), 381–392.

СПИСОК ЛИТЕРАТУРЫ

1. **Huard S.** Polarization of light. Chichester, UK: John Wiley & Sons, Inc., 1997. 352 p.

2. **Ищенко Е. Ф., Соколов А. Л.** Поляризационная оптика. 3-е изд., испр. и доп. М.: Физматлит, 2019. 576 с.

3. **Аззам Р., Башара Н.** Эллипсометрия и поляризованный свет. Пер. с англ. М.: Мир, 1981. 584 с.

4. **Джеррард А., Бёрч Дж. М.** Введение в матричную оптику. Пер. с англ. М.: Мир, 1978. 344 с.

5. **Ярив А., Юх П.** Оптические волны в кристаллах. Пер. с англ. М.: Мир, 1987. 616 с.

6. **Collett E.** Polarized light in fiber optics. Bellingham, Washington, USA: SPIE Press, 2003. 540 p.

7. **Temkina V., Medvedev A., Mayzel A.** Research on the methods and algorithms improving the measurements precision and market competitive advantages of fiber optic current sensors // Sensors. 2020. Vol. 20. No. 21. P. 5995.

8. **Крылов Г. М., Фатьянов О. В., Дуплинский А. В.** Влияние стыков двулучепреломляющего волокна на дрейф видности в интерферометре Маха – Цендера // Квантовая электроника. 2020. Т. 50. № 5. С. 447–453.

9. **Temkina V., Medvedev A., Mayzel A., Sivolenko E.** Quarter wave plate for fiber optic current sensor: Comparison of modeling and experimental study // International Youth Conference on Electronics, Telecommunications and Information Technologies (Proceedings of the YETI 2021, St. Petersburg, Russia). Edited by E. Velichko, V. Kapralova, P. Karaseov, et al. Book Series “Springer Proceedings in Physics”. Vol. 268. Springer Cham, 13 January, 2022. Pp. 437–448.

10. **Молчанов В. Я., Скроцкий Г. В.** Матричный метод вычисления собственных состояний поляризации анизотропных оптических резонаторов (обзор) // Квантовая электроника. 1971. № 4. С. 3–26.

11. **Yang J., Yu Z., Yuan L.** Characterization of distributed polarization-mode coupling for fiber coils // Peng G. D. (Ed.). Handbook of Optical Fibers. Singapore: Springer Nature Singapore Pte. Ltd., 16 May 2018. 40 p.

12. **Wuilpart M., Megret P., Blondel M., Rogers A. J., Defosse Y.** Measurement of the spatial distribution of birefringence in optical fibers // IEEE Photonics Technology Letters. 2001. Vol. 13. No. 8. Pp. 836–838.

13. **Rashleigh S.** Origins and control of polarization effects in single-mode fibers // Journal of Lightwave Technology. 1983. Vol. 1. No. 2. Pp. 312–331.

14. **Kells L. M., Kern W. F., Bland J. R.** Plane and spherical trigonometry. Warsaw: Andesite Press, 2017. 526 p.

15. Polarization Maintaining (PM) Patch Cord 980, 1030, 1064, 1310, 1550 nm. Режим доступа: https://www.afwtechnologies.com.au/pm_patchcord.html (Дата обращения: 27. 07. 2023).

16. 1550 nm Polarization Maintaining Patch-cord // Режим доступа: https://www.dkphotonics.com/product/1550nm-polarization-maintaining-patch-cord.html (Дата обращения: 27.07.2023).

17. **Fedotov A., Ustimchik V., Rissanen J., Kolosovskii A., Voloshin V., Vorob’ev I., Gumenyuk R., Chamorovskiy Y., Filippov V.** Active tapered double-clad fiber with low birefringence: supplement // Optics Express. 2021. Vol. 29. No. 11. Pp. 16506–16519.

18. **Tentori D., Garcia-Weidner A., Kuzin E.** On the birefringence evaluation of single-mode fibers // Revista Mexicana de Fisica. 2016. Vol. 62. No. 4. Pp. 381–392.

THE AUTHORS

TEMKINA Valentina S.
Peter the Great St. Petersburg Polytechnic University
29 Politechnicheskaya St., St. Petersburg, 195251, Russia
temkina_vs@spbstu.ru
ORCID: 0000-0003-2083-8989

LIOKUMOVICH Leonid B.
Peter the Great St. Petersburg Polytechnic University
29 Politechnicheskaya St., St. Petersburg, 195251, Russia
leonid@spbstu.ru
ORCID: 0000-0001-5988-1429

ARCHELKOV Arseniy B.
Peter the Great St. Petersburg Polytechnic University
29 Politechnicheskaya St., St. Petersburg, 195251, Russia
arsarch11@gmail.com
ORCID: 0009-0007-4713-1293

BUCHILKO Igor R.
Peter the Great St. Petersburg Polytechnic University
29 Politechnicheskaya St., St. Petersburg, 195251, Russia
igor.buchilko@gmail.com
ORCID: 0000-0001-8179-8648

MEDVEDEV Andrei V.
Peter the Great St. Petersburg Polytechnic University
29 Politechnicheskaya St., St. Petersburg, 195251, Russia
medvedev@rphf.spbstu.ru
ORCID: 0000-0001-7083-9184

PETROV Aleksandr V.
Peter the Great St. Petersburg Polytechnic University
29 Politechnicheskaya St., St. Petersburg, 195251, Russia
alexandr-petroff1994@yandex.ru
ORCID: 0000-0001-5216-6588

СВЕДЕНИЯ ОБ АВТОРАХ

ТЕМКИНА Валентина Сергеевна – *аспирантка Высшей школы прикладной физики и космических технологий Санкт-Петербургского политехнического университета Петра Великого.*
195251, Россия, г. Санкт-Петербург, Политехническая ул., 29
temkina_vs@spbstu.ru
ORCID: 0000-0003-2083-8989

ЛИОКУМОВИЧ Леонид Борисович – *доктор физико-математических наук, профессор Высшей школы прикладной физики и космических технологий Санкт-Петербургского политехнического университета Петра Великого.*
195251, Россия, г. Санкт-Петербург, Политехническая ул., 29
leonid@spbstu.ru
ORCID: 0000-0001-5988-1429

АРЧЕЛКОВ Арсений Борисович – *студент Института электроники и телекоммуникаций Санкт-Петербургского политехнического университета Петра Великого.*
195251, Россия, г. Санкт-Петербург, Политехническая ул., 29
arsarch11@gmail.com
ORCID: 0009-0007-4713-1293

БУЧИЛКО Игорь Романович – *аспирант Высшей школы прикладной физики и космических технологий Санкт-Петербургского политехнического университета Петра Великого.*
195251, Россия, г. Санкт-Петербург, Политехническая ул., 29
igor.buchilko@gmail.com
ORCID: 0000-0001-8179-8648

МЕДВЕДЕВ Андрей Викторович – *кандидат физико-математических наук, доцент Высшей школы прикладной физики и космических технологий Санкт-Петербургского политехнического университета Петра Великого.*
195251, Россия, г. Санкт-Петербург, Политехническая ул., 29
medvedev@rphf.spbstu.ru
ORCID: 0000-0001-7083-9184

ПЕТРОВ Александр Викторович – *кандидат физико-математических наук, доцент Высшей школы прикладной физики и космических технологий Санкт-Петербургского политехнического университета Петра Великого.*
195251, Россия, г. Санкт-Петербург, Политехническая ул., 29
alexandr-petroff1994@yandex.ru
ORCID: 0000-0001-5216-6588

Received 19.06.2023. Approved after reviewing 02.08.2023. Accepted 02.08.2023.
Статья поступила в редакцию 19.06.2023. Одобрена после рецензирования 02.08.2023. Принята 02.08.2023.